ISBN: 978-3-95450-214-1 ISSN: 2673-5490 doi:10.18429/JACoW-IPAC2021-WEPAB169

TOWARDS ULTRA-SMOOTH ALKALI ANTIMONIDE PHOTOCATHODE EPITAXY

E. J. Montgomery†, C. Jing, S. Poddar, Euclid Beamlabs, LLC, Bolingbrook, IL 60440, USA
O. Chubenko, G. S. Gevorkyan, S. S. Karkare, P. Saha, ASU, Tempe, AZ 85287, USA
H. A. Padmore, LBNL, Berkeley, CA 94720 USA
R. G. Hennig, J. T. Paul, University of Florida, Gainesville, FL 32611, USA

Abstract

Photocathodes lead in brightness among electron emitters, but transverse momenta are unavoidably nonzero. Ultra-low transverse emittance would enable brighter, higher energy x-ray free-electron lasers (FEL), improved colliders, and more coherent, detailed ultrafast electron diffraction/microscopy (UED/UEM). Although high quantum efficiency (QE) is desired to avoid laser-induced nonlinearities, the state-of-the-art is 100 pC bunches from copper, 0.4 mm-mrad emittance. Advances towards 0.1 mm-mrad require ultra-low emittance, high QE, cryo-compatible materials. We report efforts towards epitaxial growth of cesium antimonide on lattice matched substrates. DFT calculations were performed to downselect from a list of candidate lattice matches. Co-evaporations achieving >3% QE at 532 nm followed by atomic force and Kelvin probe microscopy (AFM and KPFM) show ultra-low 313 pm rms (root mean square) physical and 2.65 mV rms chemical roughness. We simulate roughness-induced mean transverse energy (MTE) to predict <1 meV from roughness effects at 10 MV/m in as-grown optically thick cathodes, promising low emittance via epitaxial growth.

INTRODUCTION

Among promising low mean transverse energy (low emittance) photocathodes with high quantum efficiency (QE), bialkali K_2CsSb is a leading candidate alongside other alkali antimonides like cesium antimonide (Cs_3Sb). Historically, disordered sequentially-evaporated bialkali films exhibited root mean square (rms) surface height variation as high as 25 nm with ~100 nm periodicity; in photoinjectors with 10-20 MV/m applied fields this could spoil emittance [1]. A breakthrough effort on co-evaporation achieved near atomically smooth surfaces, out-of-plane roughness of 0.6 nm rms, and nearest neighbor peak spacing of 40 nm [2]. In-situ atomic force and Kelvin probe microscopies (AFM/KPFM) still more recently were implemented to characterize single-alkali cesium antimonide nano-roughness [3] and identify a 25-30 meV surface roughness contribution to MTE. Measured chemical roughness of ~100 mV with 100 nm periodicity dominated the MTE contribution at low field, while in moderately high gradients >10 MV/m, physical roughness dominated.

LATTICE MATCHING AND DFT

In pursuit of lattice-matched epitaxy, an in-depth survey was performed of 150 candidate substrates lattice-matched to Cs_3Sb for (001), (110), and (111) Cs_3Sb crystal faces. Inputs to the process were from the Materials Project database and compiled by the Center for Bright Beams. The initial list of 150 allowed strain of up to 10%, which for optically thick cathodes would be problematic. Candidates were down-selected on strain, availability of single crystals (stepped surfaces preferred), vapor pressure at cleaning and growth temperatures, substrate roughness achievable, material purity available, and number of Cs_3Sb unit cells per lattice match period (1 preferred). The results identified a subset of candidates: several single crystal metals and two insulators.

Of the metals, gold was ruled out as it readily alloys with cesium, ruthenium had a less than optimal three-unit-cell match, and commercially polished niobium had >10Å rms roughness. We down-selected to four candidates by requiring <2% strain, excellent single-crystal availability, and non-reactivity with alkali antimonide: $SrTiO_3$, TiO_2, MgF_2, and Ag.

We performed DFT relaxations for the crystalline bulk structures and interface slabs to determine the formation energy of various interface configurations between the substrates and an atomic layer of Cs_3Sb and systematically identify stable interface structures. Thin film slab models held the substrate lattice constant and allowed Cs_3Sb to relax within ± 20 % strain.

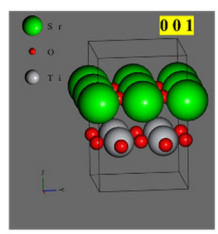

E_{cutoff} = 48.0 Ry
Equilibrium Å = 3.93114,
k-grid = 6X6X6
Equilibrium Energy = -286.43859 Ry

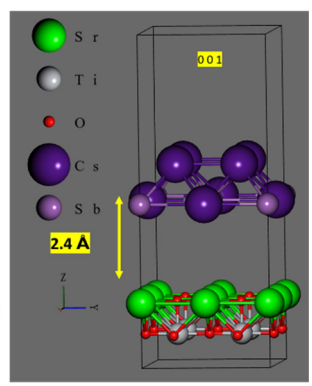

Interface	Separation between Unit Cell	$E_{interface}$ (Ry)	Formation Energy (Ry)
0.5/0.5 Sr-O/Cs-Sb	2.4 Å	-1847.0089737186	0.033976

Figure 1: Model for Sr-terminated STO (bulk, left) and Cs3Sb/STO with 2.4 Å vacuum gap, and 2:1 supercell (right). (A better lattice match exists for 7:3.) Analogous work for TiO2, MgF2, and Ag is in Table 1.

† e.montgomery@euclidtechlabs.com

ISBN: 978-3-95450-214-1 ISSN: 2673-5490 doi:10.18429/JACoW-IPAC2021-WEPAB169

The open-source software package Quantum Espresso was run on a 40-core Linux Beowulf cluster. The most lattice-matched stable compound was $SrTiO_3$, abbreviated STO. A typical DFT result is shown in Fig. 1. Calculations in bulk and heterostructures used the PWscf code of the Quantum Espresso package [4]. The ultra-soft pseudo-potential with RRKJ3 scheme was used to calculate the interaction between the atom core and valence electrons. The exchange and correction between electrons were calculated by the Perdew–Burke–Ernzerhof (PBE) in the scheme of generalized gradient approximation (GGA) [5, 6]. For the Brillouin zone integration, we used an 8×8×8 k-point mesh for the three-dimensional infinite periodic structures, and an 8x8x1 mesh for the slab structures. During the self-consistency cycles, the cut-off energy, defining the plane wave basis set, was chosen after multiple convergence tests. For STO the cutoff energy was 48 Ry (Fig. 2). The convergence tolerance was 10^{-7} eV/atom. Surfaces were constructed using a supercell with a thin slab separated from its periodic images by a vacuum layer, sized such that there are always ~ 20 Å of vacuum between the surfaces. All the atomic modelling for thin slabs was performed in BURAI [7], a free interface for Quantum Espresso. The lattice cleavage was performed using VESTA [8]. Steps were:

1. Calculate bulk SCF energy for converged lattice constants.
2. Calculate bulk slab energy for periodic slab models given surface termination and crystallographic axis.
3. Form the heterojunction interface and calculate energy of formation vs Cs_3Sb lattice constant.

The lattice mismatch appears as strain in the alkali antimonide layer since the substrates are allowed no relaxation.

Plots from the third step for the STO model of Fig. 1 are shown below in Fig. 2.

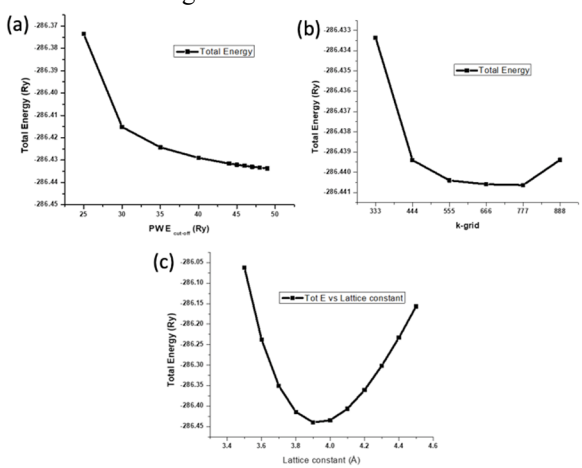

Figure 2: Bulk calculations (step 1) for (001) STO: (a) plane wave energy cutoff (48 Ry selected), (b) total energy versus size of the k-grid (6x6x6 selected), (c) total energy vs STO lattice constant (-286.44 Ry at 3.93 Å).

The strain was calculated as $\frac{\mathbf{d}_{\mathbf{substrate}} - \mathbf{d}_{\mathbf{Cs3Sb}}}{\mathbf{d}_{\mathbf{substrate}}}$ where d is the lattice constant. A positive value indicates tensile and negative value indicates compressive strain. For STO, which has a perovskite structure with Sr atoms at the vertices of the cube, O atom at the face centers which form an octahedral cage, and the Ti atom in the body center, the equilibrium lattice constant is 3.93 Å as shown in Fig. 2. Equilibrium lattice constant d for bulk Cs3Sb is 9.334 Å. For the interface, a super cell of half unit cells (2x2) SrTiO3 with half unit cell (1x1) Cs_3Sb was used as shown Fig. 1. The compressive strain for the Cs3Sb layer was found to be roughly -0.18 for the 2:1 lattice match, and -.015 for the 7:3 lattice match with STO.

The formation energy as applied to the interfaces is a measure of the stability when two dissimilar surfaces are brought together to form an interface. It considers the hybridization and charge transfer that takes place in the local density of states of the overlapping orbitals near the surface. A positive value means the surface will likely form with higher values indicating a stable interface. A negative value on the other hand indicates the interface not being energetically favorable. The formation energy for each heterostructure and the compressive strain on Cs_3Sb is summarized in Table 1.

Table 1: Summary of DFT Analysis

Substrate	d (Å)	Supercell Ratio	Formation Energy (Ry)	Predicted Strain
$SrTiO_3$ (001)	3.931	2:1*	0.03398*	-0.18*
TiO_2 (001)	4.608	2:1	0.5155	-0.013
MgF_2 (001)	4.676	2:1	0.05780	+0.0019
Ag (001)	4.158	2:1	-0.02266	-0.12

*Initial Sr-teminated STO simulation used a conservative 2:1 supercell; estimated strain using Material Project parameters was only -0.015 for a 7:3 supercell but was too computationally intensive for the 40-core cluster available in DFT work.

Titanium dioxide and magnesium fluoride (MgF_2) interfaces with Cs_3Sb were predicted to be stable as well, but, STO was preferred since it was commercially available with 1 Å rms roughness. MgF_2 had the best lattice match but only 5Å rms roughness. In STO, it is simple to prepare an atomically stepped <1Å rms surface with a 2-hr 600ºC surface reconstruction. The STO can be niobium-doped for conductivity and Sr-terminated or Ti-terminated. As a control substrate with similar nanoscale flatness but without lattice-matching, atomically-stepped heavily-doped silicon was chosen.

ROUGHNESS MEASUREMENTS

Experimental techniques are detailed separately in these proceedings [6]. STO substrates used SrTiO3 (001) single cystal, 10 x 10 mm, with 0.5 mm thickness and 0.05% Nb doping by weight, single side polished. The surface finish was guaranteed better than 5 Å rms, and the (100) orientation was good to ±0.5º. It was grown via a Vernueil process,

ISBN: 978-3-95450-214-1 ISSN: 2673-5490 doi:10.18429/JACoW-IPAC2021-WEPAB169

and the resistivity with Nb doping was 0.1 Ohm-cm. AFM showed atomic steps and gave a consistent terrace height of .3 nm, and the forward and reverse scans matched. After a 2-hr 600ºC anneal, growth proceeded for 2 hrs via co-deposition of Sb and Cs to peak 532 nm QE of 3.2%. Physical and chemical rms roughnesses were assessed via in-situ AFM and KPFM at 313.2 pm and 2.653 mV respectively. Out-of-plane AFM periodicity was ~60 nm for thin films and ~100 nm for optically thick films, while KPFM periodicity was uncorrelated with AFM and appears indicative of only one or two crystal faces and surprising work function uniformity in Cs_3Sb [9].

A subsequent set of growths plotting roughness vs Cs-Sb film thickness on both STO and Si were performed, (see Fig. 4 of Saha et al., this conference [9]). The epitaxial growth of Cs-Sb roughens faster as a function of epilayer thickness when co-evaporated on non-lattice-matched Si compared to STO. For optically thick cathodes STO provided a 3x improvement in rms physical and 4x improvement in rms chemical roughness.

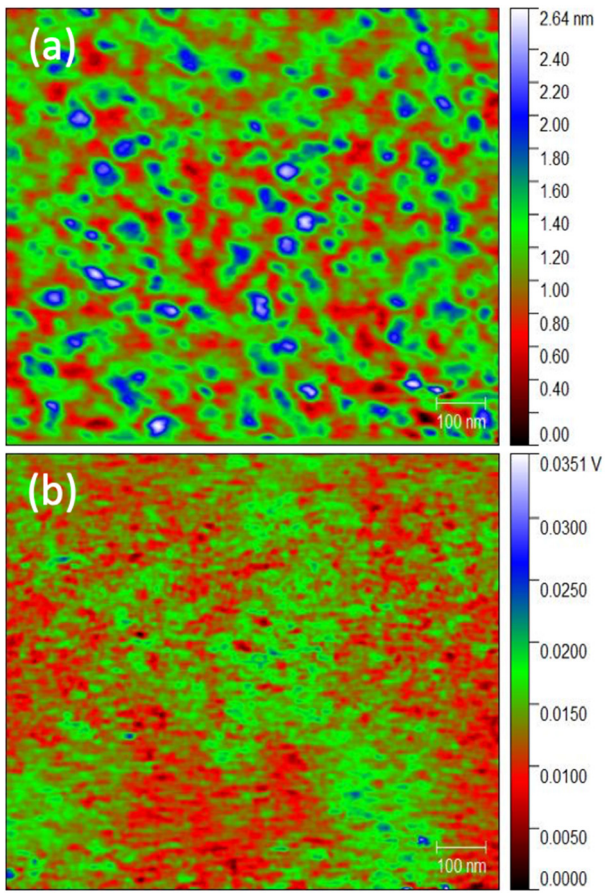

Figure 3: (a) AFM scan 0.72x1.00 µm, (b) KPFM.

EFFECT ON MTE

Using an equipotential approach, Gevorkian et al. reported a formalism for calculating mean transverse energy (MTE) using measured surface roughness maps from AFM and KPFM [3]. For each value of the external longitudinal applied electric field E, a quasi-Fourier decomposition of the local potential is performed which obeys Gauss' Law, and the electrons are tracked starting with zero velocity. The total MTE for the rough surface is subtracted from total MTE of an ideal flat surface to identify the roughness-induced MTE contribution. For a typical rough co-evaporated Cs3Sb cathode, this is of order 30 meV, with a minima near 10 MV/m. Performing the calculation on the as-grown lattice-matched co-evaporation maps in Fig. 3, the partial contribution to MTE from roughness is predicted versus applied DC electric field in Fig. 4. Note the vertical axis is the roughness-induced contribution to MTE, not to be confused with total MTE. MTE contributed by roughness is predicted to be negligibly small, <1 meV.

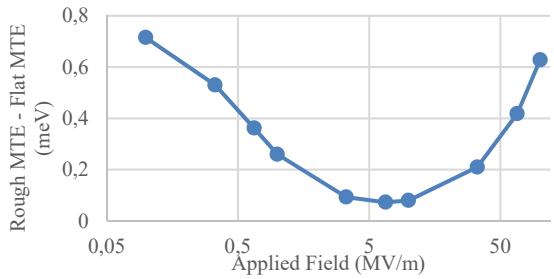

Figure 4: The part of MTE attributed to roughness effects using measured AFM and KPFM maps, compared to an ideal flat emitter.

CONCLUSION AND FUTURE WORK

We have produced near-atomically smooth and perhaps the most chemically uniform cesium antimonide cathodes to date, with a prediction of <1 meV contribution to total MTE from surface roughness effects at 10 MV/m. Future work will emphasize repeatability and optimization of deposition parameters, and will measure DC-gun emittance at cryogenic temperatures. Numerical study of MTE contributions from surfaces with comparable physical and chemical rms roughness but divergent distributions is motivated.

ACKNOWLEDGEMENTS

This work was supported by U.S. Department of Energy, Office of Science, Office of Basic Energy Sciences, under grant number DE-SC0020575. Additional funding came from the U.S. National Science Foundation award PHY-1549132 to the Center for Bright Beams, as well as DOE grant number DE-SC0021092.

REFERENCES

[1] J. Smedley *et al.*, "Sputter Growth of Alkali Antimonide Photocathodes: An in Operando Materials Analysis", in *Proc. 6th Int. Particle Accelerator Conf. (IPAC'15)*, Richmond, VA, USA, May 2015, pp. 1965-1967. doi:10.18429/JACoW-IPAC2015-TUPHA003

[2] J. Feng, S. Karkare, J. Nasiatka, S. Schubert, J. Smedley, and H. Padmore, "Near atomically smooth alkali antimonide photocathode thin films," Journal of Applied Physics, vol. 121, no. 4, p. 044904, Jan. 2017. doi:10.1063/1.4974363

ISBN: 978-3-95450-214-1 ISSN: 2673-5490 doi:10.18429/JACoW-IPAC2021-WEPAB169

[3] G. Gevorkyan, S. Karkare, S. Emamian, I. V. Bazarov, and H. A. Padmore, "Effects of physical and chemical surface roughness on the brightness of electron beams from photocathodes," *Physical Review Accelerators and Beams*, vol. 21, no. 9, Sep. 2018.
doi:10.1103/physrevaccelbeams.21.093401

[4] P. Giannouzzi *et al*. "QUANTUM ESPRESSO: a modular and open-source software project for quantum simulations of materials," *Journal of Physics: Condensed Matter*, vol. 21, no. 39, p. 395502, Sep. 2009.
https://quantum-espresso.org
doi:10.1088/0953-8984/21/39/395502

[5] D. Vanderbilt, "Soft self-consistent pseudopotentials in a generalized eigenvalue formalism," *Physical Review B*, vol. 41, no. 11, pp. 7892–7895, Apr. 1990.
doi:10.1103/physrevb.41.7892

[6] J. P. Perdew, K. Burke, and M. Ernzerhof, "Perdew, Burke, and Ernzerhof Reply:," *Physical Review Letters*, vol. 80, no. 4, pp. 891–891, Jan. 1998.
doi:10.1103/physrevlett.80.891

[7] Burai 1.3, https://nisihara.wixsite.com/burai

[8] K. Momma and F. Izumi, "VESTA 3for three-dimensional visualization of crystal, volumetric and morphology data," *Journal of Applied Crystallography*, vol. 44, no. 6, pp. 1272–1276, Oct. 2011. doi:10.1107/s0021889811038970

[9] P. Saha *et al.*, "Optical and Surface Characterization of Alkali-Antimonide Photocathodes", presented at the 12th Int. Particle Accelerator Conf. (IPAC'21), Campinas, Brazil, May 2021, paper THPAB142.